CLIMA 2016 - proceedings of the 12th REHVA World Congress

volume 9

Heiselberg, Per Kvols

Publication date:
2016

Document Version
Publisher's PDF, also known as Version of record

Development and tests of bionic fittings for heating nets

Karsten Tawackolian[#1], Hossein Sagheby[2], Daniel Brandt[#3], Martin Kriegel[#4]

[#]*TU Berlin, Hermann-Rietschel-Institut, Chair of Heating, Ventilation and Air Conditioning*

[1]karsten.tawackolian@tu-berlin.de, [2]kontakt@hri.tu-berlin.de,
[3]daniel.brandt@tu-berlin.de, [4]m.kriegel@tu-berlin.de

Abstract

A number of nature's developments such as evolutionarily optimized shapes, drag reducing surfaces and additives have so far not been widely used in thermal distribution networks. The BioNet project at the Hermann-Rietschel-Institut aims at adopting promising solutions to this specific application and evaluating potential energy savings in domestic thermal distribution networks. Numerical simulations (CFD) are used to adopt and evaluate the approaches to heating and cooling nets as well as to explain the physical principles of the bionic developments. An evolutionarily optimized bend shape was developed that reduces the pressure losses by about 20 % in comparison to the conventional bend. The shape can easily be manufactured and the connection geometry of the conventional fitting is preserved. The performance of the new shape is demonstrated by numerical simulations, by high precision single component pressure loss measurements and in a practical test case for a demo piping circuit with ten bends.

Keywords –pressure drop, heating system, CFD

(a) (b) (c)

Fig. 1: New bionic bend with 20 % less pressure loss
(a) bends created from PVC piping (b) 3D laser sintered fitting (c) CFD simulation

1. Introduction

If a bend is needed in a pipe net, there are in principle, two options for the engineer. One can either bend the pipe by hand or use a prefabricated fitting. Often, prefabricated fittings are used, because of the reduced construction effort and lower space requirements. Hand bent pipes can be used if there is sufficient space to accommodate a large curvature radius R_k e.g. $R_k/D > 4$.

Rechenberg developed a bionic bend with a reduced pressure loss based on the bionic principle of evolutionary optimization [1]. The bionic bend described in the original publication has a large curvature radius of R_k/D=19.74 and is therefore not directly applicable as a pipe fitting for heating nets. It is shown in [2] that in heating nets, a potential for reducing pressure losses exists for small curvature radii $R_k/D < 3$. The curvature radius of bend pipe fittings used in heating nets is not standardized because different manufacturers use different fabrication methods. Typical values of commonly available fittings range between $1<R_k/D<1.5$. A bend with R_k/D=1.5, i.e. at the upper end of this range, was selected for the current investigation, which is common in heating nets and still has a meaningful potential for improvement. Lower curvature radius bends are not further considered here since they can potentially be replaced by the larger radius alternatives.

a. Parameter Space

Heating nets are characterized by a variety of parameters that influence the fluid flow and need to be considered for a comprehensive analysis. These include pipe diameter D, temperature ϑ, fluid viscosity ν and flow velocity u or resp. flow rate Q. In the case of the pressure loss analysis of hydraulic systems, the study of pressure loss coefficients ζ can be based on the Reynolds number Re [3], [4], thereby significantly reducing the parameter space that needs to be investigated.

$$\zeta = \zeta(Re) \quad , \quad Re = \frac{u\,D}{\nu} \quad , \quad u = \frac{Q}{A} \qquad (1)$$

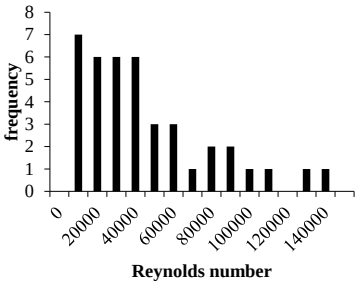

Fig. 2: Typical Reynolds numbers in heating nets that are sized according to the German standard VDI 2073

In order to find the relevant Reynolds number range in heating nets, we assessed the pipe sizing tables from the German standard VDI 2073 [5] (see Fig. 2). Reynolds numbers were calculated for temperatures of 20 °C and 70 °C. In conclusion, the typical Reynolds numbers in domestic heating nets range between 10 000 and 50 000. The literature [4], [6] shows that the influence of the Reynolds number on the pressure loss coefficient is pronounced under two conditions: (1) low loss components with a low ζ-value and (2) the intermediate Reynolds number range between 2 000 and 200 000. In our case, both conditions apply, complicating the analysis for the current conditions. Additionally, for the small diameters (16 mm and 20 mm) measured in this study, even a small change in the internal shape or surface structure of a pipe fitting causes an appreciable difference in pressure loss [7]. For small diameters, absolute values of the pressure loss coefficient can therefore only be determined for a specified type of manufacturing. As a prerequisite, the manufacturing process should ensure smooth inner wall surfaces and no additional protrusions into the flow before further optimizations are considered.

2. Method

Measurements were performed on the two test rigs depicted in Fig. 3 and Fig. 4. The inner pipe diameter on the gravimetric test rig is 21 mm, and 16 mm on the board test rig. The gravimetric test rig enables accurate measurements of ζ-values and the board test rig is used to test the performance of components for hands-on non ideal flow conditions.

a. Gravimetric test rig

Fig. 3 shows the sketch of the gravimetric test rig. The flow rate measuring principle is developed in accordance with ISO 4185. The test line is horizontal and contains the 90°-bend whose ζ-value is to be determined. At the end of the test line, the route branches in two directions. One end leads the water into the storage tank, while the other end collects the water in a smaller weighing tank for a gravimetric measurement of the mass using a precision scale. The line leading directly to the storage tank is used for long-time pressure difference measurements at the test section, as well as to ensure a fully developed flow in the pipe before the flow is switched towards the weighing tank. The switching is carried out via fast-response solenoid valves. The water in the weighing tank is circulated back into the storage tank after the measurement is carried out. To set different mass flow rates, fine regulation valves are used which are located far downstream of the test section. The static (geodesic) pressure is provided by a constant level elevated tank. It has a total capacity of 500 l and is equipped with a constant level overflow. These measures together with a long inlet section before the test section result in a very steady undisturbed flow at the test element. In that way, provided with a total head maintained at a constant level (total geodesic pressure) and a precise mass flow measurement, the gravimetric experimental design makes accurate measurements of ζ-values possible. There are several pressure measurement points up- and downstream of the tested bends. These are used to measure the pressure drop in the straight pipe as well as over the bend.

b. Board test rig

The second experimental setup (see Fig. 4) consists of two symmetric spiral circuits each containing 10 bends. One circuit includes conventional piping with bend pipe fittings; the other circuit is equipped with bionic bends. Measurements of the pressure loss can be carried out separately for each circuit at different flow rates. The circuits are built in the exact same way with the same materials and the same total length. The differences between the two measured pressure losses are assumed to only result from the different shapes of the bends. The geometric form of the circuits results in a non-fully developed flow at each bend with secondary flows. The layout represents a more hands-on installation situation. Different than the situation in the gravimetric experimental setup, which is particularly suited for exact measurements, the flows in heating networks usually have an undefined character with possible non-developed flow distributions and secondary flows. The board test rig is used to compare the new bionic bends and the conventional counterparts in such disturbed flows.

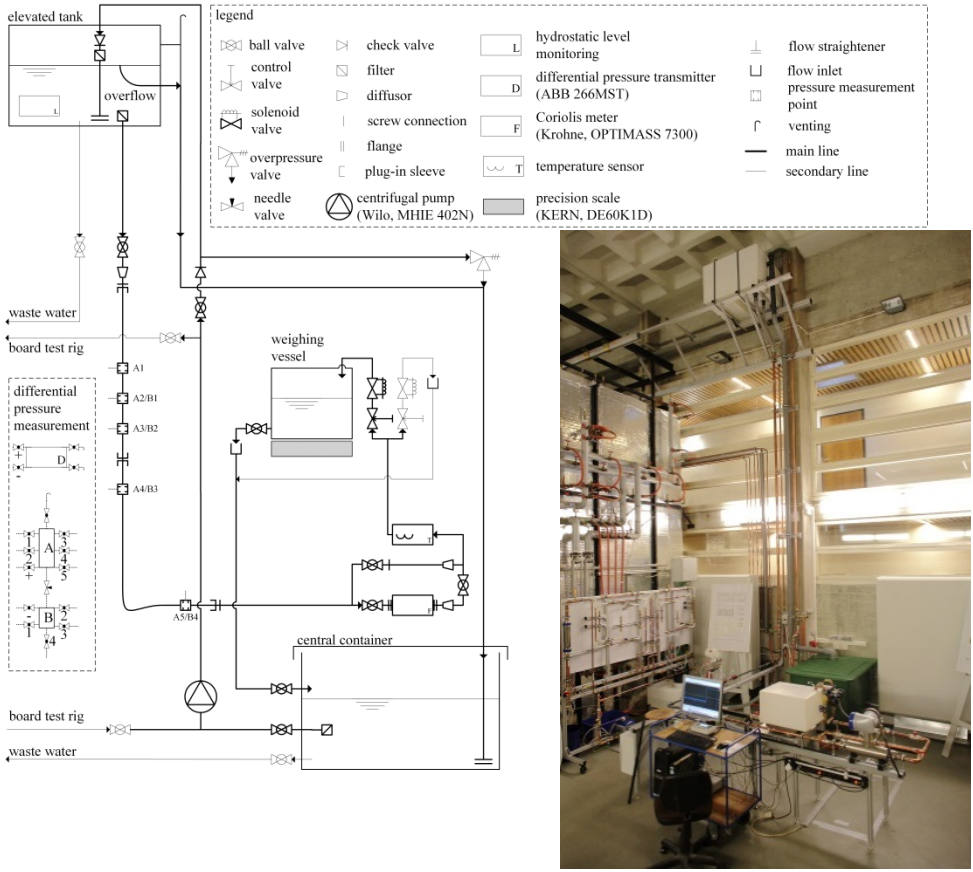

Fig. 3: Gravimetric test rig for single component measurements

Fig. 4: Board test rig of a hydraulic net with ten bends.
Left : conventional bends, right: new bionic bends.

c. Simulations

CFD simulations of the pipe fittings are carried out using STAR-CCM+ [8]. The simulation approach and verification study are documented in [2]. The simulations are based on the SST turbulence model with low-Reynolds wall resolution [9].

A **bionic bend** was parametrized as a cubic spline with three anchor points. In the first step, an evolutionary optimization study was performed for *Re*=20 000 and 100 000 to find the geometry with the lowest pressure loss. In the second step, the best geometry was simulated for a range of Reynolds numbers and compared with a simulation of the classic bend. For the **single bends**, the analysis was carried out for 18 Reynolds numbers between 2 000 and 140 000.

The **board test rig** (Fig. 5) was also simulated. In the first simulations using the SST model, a strong swirl developed at the downstream bend locations 5-10 and the phenomenon of swirl switching [10] was observed (see Fig. 6). In this case the flow symmetry breaks and one of the dean vortices dominates over the other. Strong fluctuations were also found during the measurements. Since steady flow conditions may not be realistic for such flows, future investigations will also include unsteady flow simulations. Reproducible and stable results could be obtained in the current investigation by changing the turbulence model to an elliptic blending Reynolds stress model (RSM). This suppressed the swirl switching and limited the predictions to symmetric dean vortices (Fig. 7). Swirl switching can also be suppressed if symmetry boundary conditions are used in the symmetry plane of the pipe circuit. Simulations were carried out for three different meshes as a mesh study (Table 2).

d. Calculation of pressure loss coefficients

The pressure drop Δp due to a bend contains friction and deflection losses [4]. Based on the pressure drop in a straight pipe Δp_{sp} with length L_{sp}, the fluid density ρ and the mean flow velocity u, the dimensionless friction coefficient λ is defined as

$$\lambda = \frac{D}{L_{\mathrm{sp}}} \frac{2\,\Delta p_{\mathrm{sp}}}{\rho u^2} \tag{2}$$

The pressure drop due to the bend is expressed in dimensionless form as

$$\zeta_u = \frac{2\,\Delta p}{\rho\, u^2} - \frac{L_{\mathrm{ud}}}{D} \lambda_{\mathrm{ud}} \tag{3}$$

The two pressure measurements are preferably located in undisturbed regions far upstream and downstream of the bend, resulting in the additional pipe length L_{ud}. This can only be realized with single component measurements. In the board test rig the pressure loss coefficients were calculated based on the total pressure difference at two locations ten diameters upstream and downstream of the bends. The friction due to the length of the bend L_{bend} can be subtracted to calculate the pressure drop coefficient through deflection.

$$\zeta = \zeta_u - \frac{L_{\mathrm{bend}}}{D} \lambda = \frac{2\,\Delta p}{\rho\, u^2} - \frac{L_{\mathrm{ud}}}{D} \lambda_{ud} - \frac{L_{\mathrm{bend}}}{D} \lambda_{\mathrm{bend}} \tag{4}$$

Table 1: Simulation parameters

Pipe diameter	D	20 / 16	mm
Temperature	ϑ	20	°C
Density	ρ	998.2	kg/m³
Dyn. Viscosity	η	1.0016	m Pa s
Curvature radius	R_k	1.5 D	
Reynold No.	$Re = \frac{u\,D}{\upsilon}$	20 000	
Simulation model			
Physics	Steady, isochorous		
Wall model	Low-Reynolds		
Turbulence model	SST-k-ω (single bend), Elliptic Blending Reynolds Stress (board test rig)		

Table 2 : Overview of numerical grids

	Number of cells in million
Single bends	
analysis	2.2
optimization	0.6
Pipe net	
grid 1	7.8
grid 2	14.2
grid 3	31.9

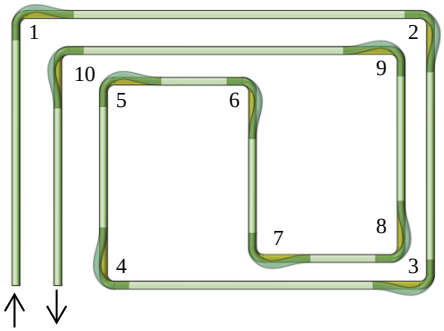

Fig. 5: Board test rig with ten bends

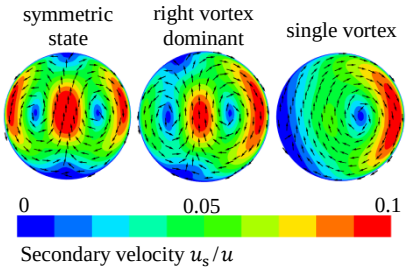

Fig. 6: Swirl switching of Dean vortices

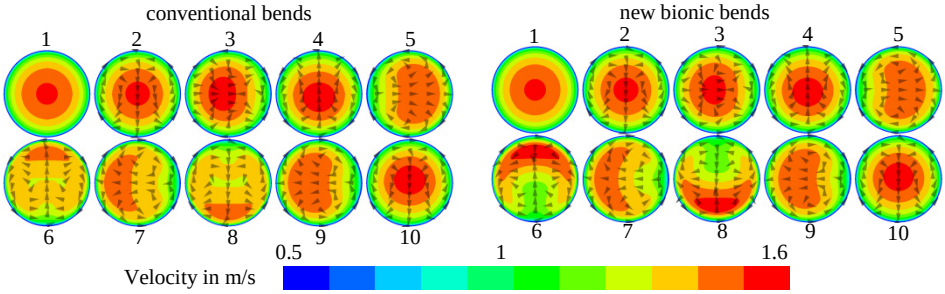

Fig. 7: Calculated velocity distribution upstream of bend 1 to 10 in the board test rig

3. Results

a. Bionic bend

In the optimization study, relatively coarse grids (0.6 million cells) were used to reduce the numerical effort. Therefore the ζ_u -value is systematically under predicted [2]. For the optimization, the ζ_u-value is calculated according to eq. 3 to include all relevant losses. It was previously determined that a finer mesh with about four times as many cells as used in the current optimization study is needed to achieve a grid independent solution. Although this is often not practical, it does not negatively affect the optimization study because the relative performance of design variants is predicted reliably [2]. In total, about 150 CFD simulations were performed as part of the optimization study. An optimal solution for D=20 mm was achieved for both Reynolds numbers with h_y=1.7 cm, where h_y is the height of the overshoot in the bionic bend geometry. In a later phase of the project a reverse installation of the bionic bend was also considered. Interestingly, it was found that the performance of the ζ_u-value is maintained for the chosen geometry h_y=1.7 cm and it may even be possible to further reduce the ζ_u-value in this case, albeit with a larger geometry than h_y=1.7 cm. Since these results were found after the fabrication of the design, this design option will be considered in a future investigation.

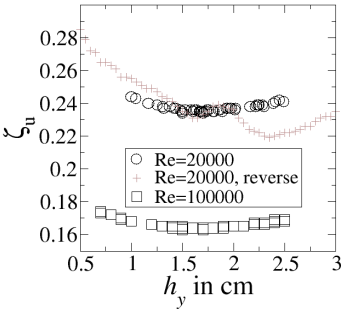

Fig. 8: Optimization of the new bionic bend for two Reynolds numbers

b. Performance comparison

The new bionic and the conventional bend were measured on both test rigs in order to validate the new design for the full range of relevant Reynolds numbers. The results seen in Fig. 10 show the ζ–value as a function of the Reynolds number. The ζ-value is calculated according to eq. 4. The measurements on the board test rig were affected by the surface roughness of the 3D laser sintered pipe fittings. A sand grain roughness of 0.06 mm (resolution of the laser sintering machine) was used to calculate the friction coefficient λ_{bend} by using the Colebrook equation [4]. The solid and dashed lines in Fig. 9 show the results with and without the roughness correction. It can be seen that the influence is dominant and leads to an appreciable uncertainty of board test rig measurements because of the necessary roughness correction.

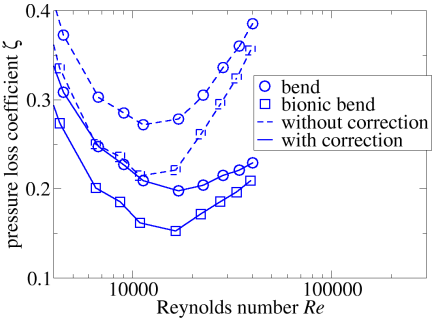

Fig. 9: Influence of surface roughness on the pressure loss coefficient for laser sintered bends

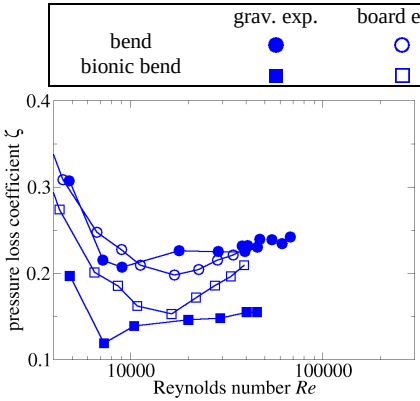

Fig. 10: Measured pressure loss coefficients

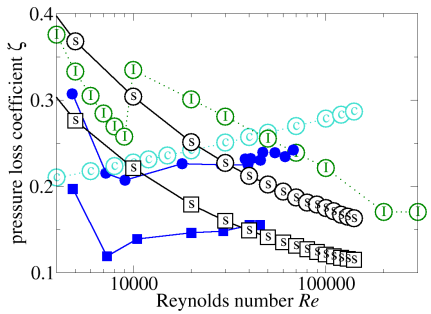

Fig. 11: Comparison of measured and simulated pressure loss coefficients

Simulations were carried out for 18 Reynolds numbers between 2 000 and 140 000. Refined grids (2.2 million cells, 50 cells in the wall region $r/R<0.5$) were used in these cases. The pressure loss coefficients are compared with empirical correlations from Idelchick [4] and Crawford [3] and the measurements on the gravimetric test rig (Fig. 11). There is a gap between the proposed curve progressions by Idelchick and Crawford for intermediate Reynolds numbers around 20 000. The correlation by Crawford suggests an increasing value for the pressure loss coefficient with the Reynolds number. In contrast, the correlation of Idelchick suggests a falling curve progression with a discontinuity at Re=10 000. As it was pointed out by Idelchick [4], the pressure loss coefficient of bends only becomes independent of Reynolds number for $Re > 2\times10^5$. For Reynolds numbers below a critical Reynolds number Re_{cr} of about 10^5, the flow separation region downstream of the bend is characterized by low levels of turbulence. The CFD simulation is based on a statistic turbulence model that cannot predict the curve progression in this transition region between Re=10 000 and Re=50 000. The inability to make predictions in this range can be attributed to the gradual transition from low turbulence to fully turbulent flow in this Reynolds number range ([4], [11]). The numerical simulation therefore predicts a too early start of the fully turbulent state and a monotonic decreasing curve progression as expected for higher Reynolds numbers. In the experiments conducted in this study, the pressure loss coefficient was measured up to Re=50 000 using the weighing system. Some additional measurements were added at higher Reynolds number up to 68 000 with a Coriolis meter as flow reference; in these cases the measured pressure loss coefficient remained nearly constant. The simulation predicts an improvement of the bionic bend for all relevant Reynolds numbers. Measurements verified this prediction for Reynolds numbers up to Re=50 000. In the experiments for very low Reynolds numbers below 10 000, the improvement is hard to show experimentally because of larger experimental uncertainties. For higher Reynolds numbers, the measured and simulated reduction of the pressure loss as expressed according to eq. 4 is approximately 23 % (see Fig. 13).

c. Pipe Circuit

The simulation results can be used to assess the dependence of the pressure loss coefficient on the installation position. The results are shown in Fig. 12. The plotted curves resulting from the three simulated mesh sizes are nearly identical. The pressure loss coefficient changes with the position of the fitting in the pipe circuit. For the

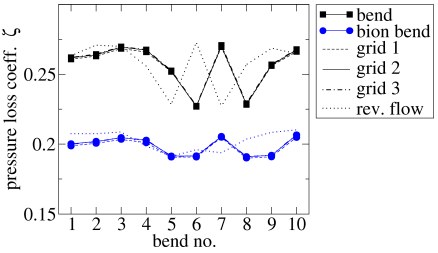

Fig. 12: Dependence of bend pressure losses on the installation position of the pipe circuits (Fig. 5). Simulation results.

bionic bend, the std. dev. is 2.4 %, and for the classic bend, 5 %. It is remarkable, that in the case of certain strong disturbances, as for example by bends 6 and 8, the pressure loss coefficient can drop considerably. A reduction of the pressure loss coefficient is observed if the flow is shifted to the outside of the bend at its inlet which is the case for bend 5, 6 and 8. This leads to slower flow velocities at the inside of the bend and a reduction of the separation zone at the inside of the bend. On the other hand, the flow separation zone increases if the flow distribution is shifted towards the inside of the bend. Except for the smaller separation zone, the calculated velocity distributions in both circuits are similar (see Fig. 7). In conclusion, it is demonstrated that the bionic bend causes lower pressure losses even if the flow conditions are disturbed. An effective reduction of pressure losses is found at all considered installation positions.

4. Conclusion

An evolutionarily optimized bend fitting shape has been presented that reduces the pressure losses by about 20 % in comparison to conventional bend fittings. The performance of the new bionic shape was demonstrated for the relevant Reynolds number range in domestic heating nets and is depicted in Fig. 13. Numerical simulations have shown good results for the optimization and evaluation of bend geometries. For the intermediate Reynolds number range, the flow physics are intricate due to an insufficiently developed turbulent state. In these conditions, simulations and experiments are prone to higher uncertainties. The performance of the new shape is demonstrated by numerical simulations, high precision single component pressure loss measurements and in a practical test case for a demo piping circuit with ten bends. The new geometry is applicable to all typical conditions in heating nets (temperature, flow rate, and diameters). Due to its simple geometry, the evolutionarily optimized bend is suitable for mass production with minimal additional costs.

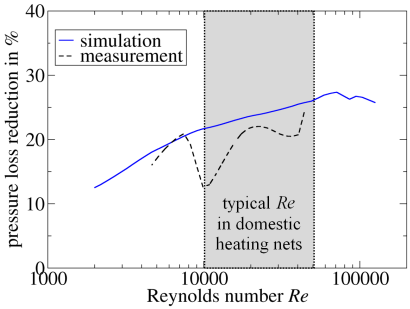

Fig. 13: Pressure loss reduction of the new bionic bend in dependence on the Reynolds number

Acknowledgements

This work is funded by the German Federal Ministry of Economics and Technology in the framework of the research program BioNet/ 03ET1197A.

References

[1] I. Rechenberg, Evolutionsstrategie 94, Stuttgart: Frommann-Holzboog, 1994.

[2] K. Tawackolian und M. Kriegel, „Numerische Simulation eines bionischen Rohrbogens für thermische Verteilnetze,“ in *BauSIM 2014-Konferenz*, Aachen.

[3] N. Crawford et al., "An experimental investigation into the pressure drop for turbulent flow in 90° elbow bends-," *Proceedings of the Institution of Mechanical Engineers, Part E: Journal of Process Mechanical Engineering*, vol. 221, no. 2, 2007.

[4] I. Idelchik, Handbook of Hydraulic Resistance (third ed.), Jaico Publishing House, 2008.

[5] *German Standard VDI 2073 Blatt 1, Nov 2012, Abschnitt 7.1, Tab. 2.*

[6] W. Wagner, Strömung und Druckverlust, Würzbuch: Vogel Buchverlag, 1997.

[7] "CIBSE Guide C: Reference Data," CIBSE, 2007.

[8] STAR-CCM+ user guide (2013),Version 10.04, 2015.

[9] D. Wilcox, Turbulence Modeling for CFD, 3rd edition, DCW Industries, Inc , 2006.

[10] C. Carlsson et al., "Swirl switching in turbulent flow through 90° pipe bends," *Physics of Fluids*, vol. 27, 2015.

[11] C. S. Lee, *Strömungswiderstände in 90°-Rohrkrümmern*, Dissertation, TU-Berlin, 1968.